Chemical Engineering Science 90 (2013) 284–298

Contents lists available at SciVerse ScienceDirect

Chemical Engineering Science

journal homepage: www.elsevier.com/locate/ces

Gasification of wood in a dual fluidized bed gasifier: Influence of fuel feeding on process performance

Stefan Kern*, Christoph Pfeifer, Hermann Hofbauer

Vienna University of Technology, Institute of Chemical Engineering, Getreidemarkt 9/166, 1060 Vienna, Austria

HIGHLIGHTS

- Gasification of wood pellets in a dual fluidized bed steam gasifier.
- Variation of feeding position of the solid feedstock.
- Improved gas yield but higher tar content by feeding of solid feedstock onto bed.
- Gas measurement at different levels in gasification reactor to study gas formation.

GRAPHICAL ABSTRACT

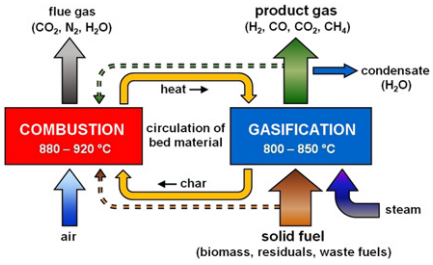

ARTICLE INFO

Article history:
Received 29 October 2012
Received in revised form
22 December 2012
Accepted 25 December 2012
Available online 4 January 2013

Keywords:
Dual fluidized bed
Gasification
Renewable energy
Fuel
Fluidization
Thermodynamics process

ABSTRACT

Gasification of wood pellets at a gasification temperature of 850 °C and a fuel power of 90 kW was performed in a dual fluidized bed gasifier. Pure steam was used as a gasification agent at a steam-to-fuel ratio of 0.6 $kg_{H_2O}/kg_{fuel,daf}$. One focus of the investigation was the influence of the position at which the solid fuel was fed into the gasifier. In one case the fuel was fed directly into the bubbling fluidized bed while in the second case the fuel was fed from the top onto the bubbling bed. With in-bed feeding much lower tar contents and a higher H_2 content were observed, while with on-bed feeding the amount of product gas generated was significantly higher. A second focus of this test series was the gas composition inside the reactor. To investigate this, gas measurements were carried out at different height levels in the reactor for both fuel feeding options. It was observed that the gas composition changed drastically along the height of the gasifier. A decrease in the H_2 content of about 12 $vol\%_{db}$ was measured from the lowest to the highest sampling point in the gasifier while the contents of higher hydrocarbons, CH_4, C_2H_4, and C_2H_6, increased towards the gasifier outlet.

1. Introduction

The worldwide demand for energy is growing and the largest part of this growth is currently covered by oil and gas. In particular the developing countries show high rates of growth connected to their growing economies (World Energy Outlook, 2010). The European Union's dependency on energy imports is expected to rise from 50% at present to around 70% in 20–30 years. In particular, the major part of natural gas is imported into the European Union from only three countries (Green Paper, 2006). As carbon dioxide emissions from biomass are perceived as being neutral, the utilization of biomass as a substitute for fossil fuels is attractive. Consequently, finding new, more effective and wide-ranging applications for low grade and cheap biogenic and fossil fuels is essential. Gasification of biomass or other solid fuels enlarges the range of its conventional application.

In many applications for gasification of solid feedstock, air is used as gasification agent, as it is cheap and drives the process autothermally. The drawback of using air is that a lot of nitrogen is introduced, dilutes the product gas, and lowers the heating

* Corresponding author. Tel.: +43 1 58801 166382; fax: +43 1 58801 16699.
E-mail address: stefan.kern@tuwien.ac.at (S. Kern).

0009-2509/$ - see front matter © 2013 Elsevier Ltd. All rights reserved.
http://dx.doi.org/10.1016/j.ces.2012.12.044

value of the product gas down to about 3–6 MJ/Nm$^3_{db}$(Zainal et al., 2002). When steam or CO_2 is used as a gasification agent, the product gas is also free of nitrogen and the calorific value of the gas is higher: for steam, gasification values between 10 and 18 MJ/Nm$^3_{db}$ can be reached (Rapagna et al., 2000; Schuster et al., 2001). The advantage using steam instead of CO_2 is that the reactivity of steam is on average about four times higher than that of CO_2 (Molina and Mondragón, 1998), so residence times of the char in the gasification section would have to be longer and the gasification efficiency would suffer. With H_2O or CO_2 as a gasification agent, the process becomes allothermal, so the heat for the endothermic gasification reactions has to be provided externally.

Dual fluidized bed (DFB) gasification solves this problem as the combustion reactor, which provides the energy for gasification, is separated from the gasification reactor and pure steam is used as gasification agent. Circulating bed material between these two reactors carries the heat from the combustion reactor to the gasification reactor. This gasification technology (Hofbauer et al., 2002) has been developed at Vienna University of Technology and has been successfully demonstrated in Güssing (Hofbauer et al., 2003) and Oberwart (Kotik, 2010), Austria, on the 8 and 10 MW_{th} scales, respectively, since 2001 and 2008. Another plant in Villach, Austria with a fuel power of 15 MW is in operation since 2011 (Klotz, 2010). Further plants in Klagenfurt, Austria, Gothenburg, Sweden (Gunnarsson, 2010), and Senden, Germany, are currently in planning (Klagenfurt), under construction (Gothenburg), or in the startup period (Senden), and will achieve fuel power of 15 MW (Senden), 25 MW (Klagenfurt), and 32 MW (Gothenburg). The Institute of Chemical Engineering at Vienna University of Technology operates a 100 kW DFB pilot plant for research purposes, where research concerning different types of biomass (Pfeifer et al., 2011a; Kitzler et al., 2011), coal (Kern et al., 2011; Kern et al., 2012a), sewage sludge (Schmid et al., 2011), or plastics (Wilk et al., 2011) as well as investigations regarding operating parameters (Kern et al., 2012b) and bed materials (Pfeifer et al., 2011b; Koppatz et al., 2011) have been carried out over the last decade.

Gasification of solid fuels in a fluidized bed reactor is an extensive matter of interest worldwide for the time being. In most of the cases of investigations there is a focus on the products (product gas composition) at the outlet of the gasification reactor, but, in particular, previous research by Miccio et al. (1999) showed that in the freeboard of a fluidized bed gasifier that uses air as a gasification agent quite a lot of reactions change the composition and yield of the product gas. For biomass gasification in fluidized bed reactors, the location where the fuel is introduced into the gasification reactor is critical (Corella et al., 2008). Gómez-Barea et al. (2013) concluded that for the case of autothermal gasification with oxygen and steam the location of fuel feeding influences the gas composition since the gas obtained if the feedstock is introduced at the top of the reactor has a pyrolytic nature compared to the case where the feedstock is fed into the middle of the bubbling bed.

The present work deals with gasification of wood pellets with pure steam as gasification agent in a dual fluidized bed gasifier operated with a fuel power of 90 kW_{th} at a gasification temperature of 850 °C. To determine the influence of the fuel feeding position, two operating points will be investigated. The first operating point deals with the fuel feeding position that introduces the feedstock directly into the bubbling bed, which is typically applied for most applications, while the second operating point outlines the influence on the system if the fuel is fed from the top onto the bubbling bed. In addition to the general reactor performance, the product gas quality, the energy flows in the reactor, and the efficiencies, gas composition measurements in the gasification reactor at different height levels of the freeboard as well as in the bubbling bed will be carried out.

2. Fundamentals

2.1. Gasification of solid feedstock with steam

The conversion of solid fuels into gaseous products by gasification occurs in several steps. The first step is drying of the fuel, followed by the release of volatile components and thermal degradation in the absence of oxygen, called pyrolysis. The residual char can be converted into product gas by a gasifying agent like air, oxygen, steam, carbon dioxide, or a mixture of oxygen and steam. In fluidized beds, gasification takes place at temperatures between 800 and 900 °C. For DFB gasification, pure steam will be used as a gasification agent, so this is the type that will be considered here.

The main gasification reactions are shown in Table 1. These reactions are considered as equilibrium reactions with changing equilibrium conditions depending on gas concentrations, temperature, and pressure. For the applied temperature range of fluidized bed gasification, equilibrium will normally not be reached. In the gasification reactor these reactions can take place at the same time and place and some reactions can be forced by operating parameters and by the utilization of catalytically active bed material. When applying steam for gasification, the water–gas shift reaction is forced, so carbon is converted into H_2 and CO (Eq. (1)), and carbon which is also present in the gas in the form of CO can be converted to H_2 and CO_2 (Eq. (2)) already in the gasification reactor. This leads to a product gas with a high content of hydrogen. Based on the gasification reactions above and including the aspect of present oxygen in the solid fuel, the overall reaction for gasification of solid fuels can be expressed as

$$C_xH_yO_z + (x-z)H_2O \rightarrow xCO + \left(x + \frac{y}{2} - z\right)H_2 \quad \text{for} \quad (x > z) \quad \Delta H_{R,850} > 0 \tag{9}$$

From Eq. (9) the minimum amount of steam that must be present during the process for a known composition of the fuel can be defined. The stoichiometric steam demand can be extracted as

$$\phi_{H_2O} = (x-z) \tag{10}$$

For the tests in this publication the feedstock can be expressed as the system $C_xH_yO_z$ free of sulfur and free of nitrogen. From the fuel analysis (see Table 2), the molarities of C, H, and O are found to be $CH_{1.44}O_{0.66}$. With the knowledge of the fuel composition, the stoichiometric steam demand can be calculated as

$$\phi_{H_2O} = 14.76\ \text{mol}_{H_2O}/\text{kg}_{\text{daf,N,S,Cl free}}$$

$$\phi_{H_2O} = 0.266\ \text{kg}_{H_2O}/\text{kg}_{\text{daf, N,S,Cl free}}$$

Table 1
Equilibrium reactions in biomass gasification according to Kaltschmitt et al. (2009).

Name of reaction	Chemical equation	ΔH[kJ/mol]	Equation
Water–gas (i)	$C + H_2O \leftrightarrow CO + H_2$	+118.5	(1)
Water–gas (ii)	$C + 2H_2O \leftrightarrow CO_2 + 2H_2$	+103	(2)
Boudouard	$C + CO_2 \leftrightarrow 2\ CO$	+159.9	(3)
Methanation	$C + 2H_2 \leftrightarrow CH_4$	−87.5	(4)
Oxidation (i)	$C + O_2 \leftrightarrow CO_2$	−393.5	(5)
Oxidation (ii)	$C + 0.5\ O_2 \leftrightarrow CO$	−123.1	(6)
Water–gas shift	$CO + H_2O \leftrightarrow CO_2 + H_2$	−40.9	(7)
Methane reforming	$CH_4 + H_2O \leftrightarrow CO + 3H_2$	+225	(8)

Table 2
Proximate and ultimate analyses of the feedstock.

Component	Unit	Wood pellets	
		Dry basis	As used
Water content		–	**6.11**
Ash content		0.29	**0.27**
C		50.23	**47.16**
H	**wt%**	6.04	**5.67**
N		0.05	**0.05**
O		43.38	**40.73**
S		0.005	**0.005**
Cl		0.003	**0.003**
Volatile matter	**wt%**	86.45	**81.17**
Fixed carbon		13.55	**12.72**
LHV	**[MJ/kg]**	18.75	17.46

In real gasifiers the water introduced for conversion of the feedstock will not be converted completely, as a result of several facts. On the one hand, to maintain a good fluidization, a steam flow higher than that required stoichiometrically is typically chosen. On the other hand the aspects discussed before only consider the conversion of the feedstock to H_2 and CO. In a real case many simultaneous reactions take place, such as pyrolysis, gasification, reforming, and cracking as well as recombination reactions for tar compounds that lead to the actual product gas composition.

From the facts mentioned above it can be assumed that the water–gas shift reaction takes place in the reactor. In general, this reaction is desired, as a high hydrogen content is welcome in many cases. Moreover, materials that promote this reaction also force the decomposition of tar compounds (Kirnbauer et al., 2012) and reduce the energy required for the process due to its exothermic character (Eq. (7)). To quantify the distance to equilibrium, a model parameter is introduced which is defined as the logarithm of the ratio of the actual partial pressure product to the equilibrium constant (Eq. (11)). If $p\delta_{\mathrm{eq,CO-shift}} < 0$, the actual state is still on the side of the reactants, so further reaction is thermodynamically possible. If $p\delta_{\mathrm{eq,CO-shift}} = 0$, the water–gas shift equilibrium is fulfilled by the product gas composition, and if $p\delta_{\mathrm{eq,CO-shift}} > 0$, the actual state is on the side of the products. The latter case cannot be reached thermodynamically by the water–gas shift reaction, but is a result of the products of devolatilization and the other gasification reactions and the water content in the product gas. If, for example, the gasifier is operated with a low amount of steam for gasification, the water content will be lower in the product gas. This moves the distance to water–gas shift equilibrium beyond 0 ($p\delta_{\mathrm{eq,CO-shift}} > 0$). The water–gas shift reaction will then move towards its reactants and consume energy

$$p\delta_{\mathrm{eq,CO-shift}}(p_i,T) = \log_{10}\left[\frac{\prod_i p_i^{\nu_i}}{K_{p,\mathrm{CO-shift}}(T)}\right] \tag{11}$$

$K_{\mathrm{P,CO-shift}}$ is the equilibrium constant of the water–gas shift reaction and can be determined via several sources (HSC, 2002). For practical operation of gasifiers an easier expression of the amount of steam is used. The steam-to-fuel ratio expresses the sum of water present in the system in relation to the total mass of dry and ash free fuel introduced (Eq. (12)). As the steam is initially required for gasification of carbon particles (Eqs. (1) and (2)) the formulation of the so-called steam-to-carbon ratio will also be used here (Eq. (13)). This formulation makes it easier to compare the gasification of fuels from with different origins, like coal and biomass, because due to the high heating value of coal compared to wood, the amount of coal required to reach the same fuel power is smaller than the amount of wood. This would result in very different steam-to-fuel ratios, but a constant steam-to-carbon ratio is essential for maintaining comparable gasification conditions

$$\varphi_{\mathrm{SF,wt}} = \frac{\dot{m}_{\mathrm{steam}} + \nu_{\mathrm{H_2O}} \cdot \dot{m}_{\mathrm{fuel}}}{(1-\nu_{\mathrm{H_2O}}-\nu_{\mathrm{ash}}) \cdot \dot{m}_{\mathrm{fuel}}} \tag{12}$$

$$\varphi_{\mathrm{SC,wt}} = \frac{\dot{m}_{\mathrm{steam}} + \nu_{\mathrm{H_2O}} \cdot \dot{m}_{\mathrm{fuel}}}{\nu_{\mathrm{C}} \cdot \dot{m}_{\mathrm{fuel}}} \tag{13}$$

In steam gasification, the amount of water introduced that is consumed for the gasification and steam reforming reactions is an indicator for the whole process. This value is called water conversion. The relative water conversion is defined as the amount of water consumed per mass unit of converted fuel

$$X_{\mathrm{H_2O,rel}} = \frac{\dot{m}_{\mathrm{H_2O,con.}}}{(1-\nu_{\mathrm{H_2O}}-\nu_{\mathrm{ash}}) \cdot \dot{m}_{\mathrm{fuel}}} \tag{14}$$

The absolute water conversion simply expresses the relation between the amount of water consumed and the amount of water introduced as

$$X_{\mathrm{H_2O}} = \left(\frac{\dot{m}_{\mathrm{H_2O,con.}}}{\nu_{\mathrm{H_2O}} \cdot \dot{m}_{\mathrm{fuel}} + \dot{m}_{\mathrm{H_2O,steam}}}\right) 100 \tag{15}$$

The conversion of carbon in the gasifier to gaseous products can also be used as a key figure for the performance of the gasification process. This value is the carbon conversion. For a dual fluidized bed gasifier, one has to distinguish between the conversion of carbon to product gas in the gasification reactor itself and the conversion of carbon in the whole system to product gas and flue gas. In the first case, the carbon conversion is the ratio of carbon leaving the gasification reactor in the form of gaseous products in the product gas stream to the amount of carbon introduced by the feedstock

$$X_C = \left(\frac{\dot{m}_{C_{\mathrm{PG}}}}{\nu_C \cdot \dot{m}_{\mathrm{fuel}}}\right) 100 \tag{16}$$

X_C can be used as a kind of parameter for determination of the amount of char that leaves the gasification reactor and enters the combustion reactor, neglecting char present in the product gas stream.

2.2. Olivine as bed material

During the last few years, olivine has become a widely known and used bed material and in-bed catalyst for fluidized bed gasification. It is a naturally occurring mineral formed of silicate tetrahedra which contain iron and magnesium $(Mg_{1-X}, Fe_X)SiO_2$. The content of iron and magnesium usually differs depending on where the olivine has been mined. The effect of catalytic tar reduction through the use of olivine as a bed material was reported by Koppatz et al. (2011). Calcination of the olivine before using it can greatly improve its catalytic activity (Devi et al., 2005). For long-term utilization of olivine in biomass gasification systems, Kirnbauer, Hofbauer (2011) investigated the interaction of the fuel ash with the olivine particles to form layers, rich in calcium, around the particles. The effect on the gasification process is that the catalytic effect is considerably improved, so the GC/MS tar values were found to be around 80% lower and the gravimetric tar produced was approximately 65% lower in the operation with coated olivine particles compared to the operation using fresh, uncoated olivine particles (Kirnbauer et al., 2012).

3. Materials and methods

3.1. The dual fluidized bed pilot plant at Vienna University of Technology

For pilot scale experiments, Vienna University of Technology operates a 100 kW dual fluidized bed (DFB) gasification reactor (Pfeifer et al., 2011a). A schematic drawing of the pilot rig is shown in Fig. 1. The fuel, usually biomass, enters the gasification reactor, a bubbling bed fluidized with steam, where drying, pyrolysis, and heterogeneous char gasification takes place. The remaining residual char leaves the gasification reactor at the bottom together with bed material, which circulates between the two reactors, through the lower loop seal to the combustion reactor. This reactor is designed as a fast fluidized bed that is fluidized with air to maintain combustion of the residual char and additional fuel, if required. By burning char and additional fuel in the combustion reactor, the bed material is heated up, and after particle separation from the flue gas at the exit of the combustion reactor, the bed material flows back to the gasification reactor via the upper loop seal. Both the lower and upper loop seals are fluidized with steam to ensure a high throughput of bed material and to avoid any leakage of gas between the reactors. In practical operations, the gasification temperature is normally controlled by the addition of fuel (e.g. recycled producer gas, part of the feedstock, etc.; Fig. 1, fuel to comb.) into the combustion reactor. In the case of the 100 kW pilot plant, light heating oil is used as fuel in the combustion reactor as it is easy to handle in pilot scale processes. The main basic geometry data of the DFB reactor system are summarized in Koppatz et al. (2011).The process yields two separate gas streams at high temperatures: a high quality producer gas and a conventional flue gas.

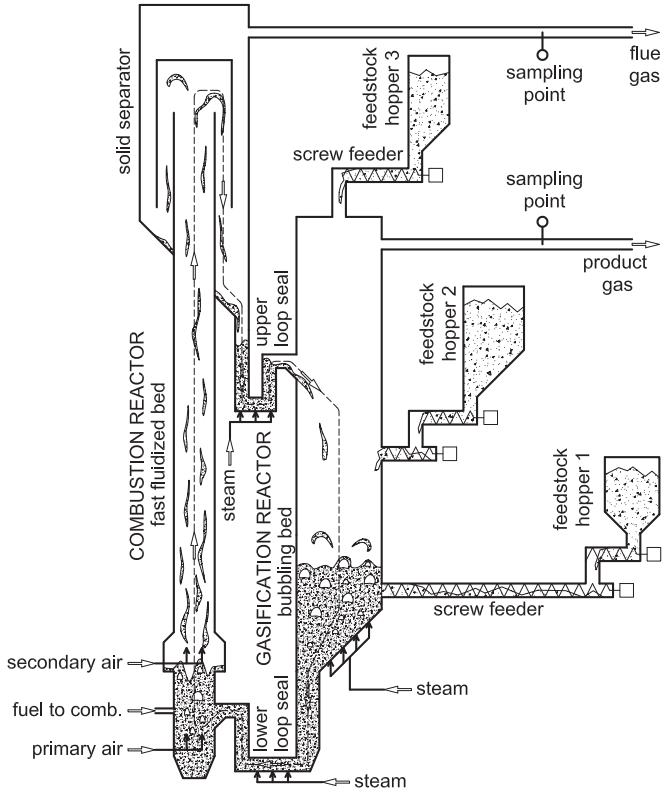

Fig. 1. Scheme of the dual fluidized bed gasification pilot plant at Vienna University of Technology.

The pilot plant is equipped with three different hoppers to enable fuel to be fed into the gasification reactor at different locations as well as to give the possibility of co-gasification of several feedstock at any mixing ratio. The three hoppers are used for the following feeding locations or fuel requirements:

- Hopper 1: for feeding of solid fuels into the bubbling bed of olivine particles. The screw conveyor introduces the fuel about 0.3 m below the splash zone of the bubbling bed. In most cases this hopper is used.
- Hopper 2: for feeding of solid fuels from the side into the freeboard of the gasifier. The screw conveyor introduces the fuel about 0.3 m above the splash zone of the bubbling bed.
- Hopper 3: for feeding of solid fuels from the top of the gasifier (top-down feeding). This feeding position is designed for fuels with a low melting point like plastics and ensures that the fuels do not come into contact with hot surfaces (free-falling into the reactor) before making contact with the hot bed material.

For the experiments discussed later in this article, only hopper 1 and hopper 2 were used.

3.2. Analytics

3.2.1. Measurement of main product gas composition

The composition of product gas is measured after the gasification reactor. The permanent gas components CH_4, H_2, CO, CO_2, and O_2 are measured by a Rosemount NGA 2000. The components N_2, C_2H_4, and C_2H_6 are measured using an online gas chromatograph (PerkinElmer Clarus 500). To avoid any contamination and damage of the gas analyzer and the column of the online gas chromatograph, the product gas has to be cleaned in terms of particulate matter and condensable components like higher hydrocarbons (tars) and water, as both gas measurement devices require dry gas. To maintain this, the gas cleaning line drawn in

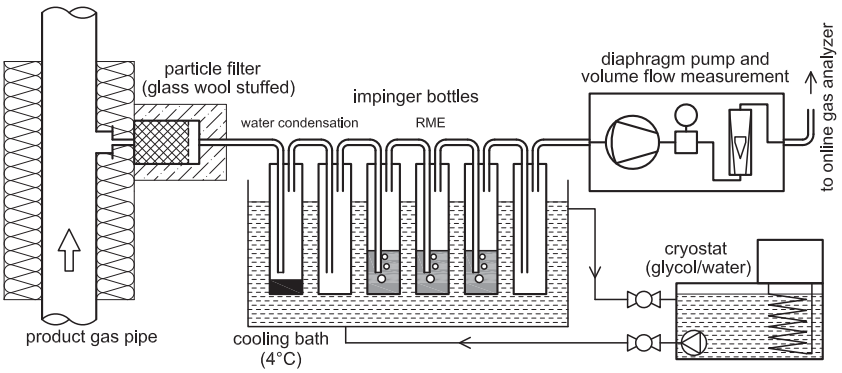

Fig. 2. Gas cleaning line for online product gas measurement.

Fig. 2 is used. Particles like dust and char are removed by a glass-wool-stuffed filter. After this particle removal the gas is led though six impinger bottles. Water and hydrocarbons that condense at temperatures higher than 4 °C are collected in the first two bottles. They are followed by three further impinger bottles. Those are filled with rapeseed oil methyl ester where tars are washed out of the gas. The last bottle ensures that no rapeseed oil methyl ester can leave the gas cleaning line accidentally and cause damage to the online gas analyzer or the online gas chromatograph.

3.2.2. Tar measurement

Tar is sampled isokinetically with impinger bottles and, afterwards, gravimetric as well as GC/MS tars are determined. The tar sampling is applied discontinuously by condensing and solving of the tar components out of the product gas. The measurement method is based on the tar protocol according to CEN/TS 15439 (Neft et al., 1999) focusing on tars originating from biomass gasification. The method applied here differs with regard to the solvent used, as CEN/TS 15439 proposes the use of isopropanol (IPA), but toluene is used here. This allows simultaneous detection of the water content in the product gas because water can be measured as a separate phase in the impinger bottles. But unlike IPA, the use of toluene as a solvent does not enable the tar components benzene, toluene, and xylene (BTX) to be detected. However, the separation performance of toluene for tar components larger than BTX is higher than that of IPA. A schematic of the arrangement of the tar sampling line is shown in Fig. 3.

The gas enters the heated sampling line, which consists of a cyclone and a glass-wool-stuffed filled filter cartridge, where dust as well as condensed tar components is deposited. Afterwards, the gas is led through six impinger bottles, five of which are filled with toluene. The impinger bottles are located in a cooling bath cooled down to -8 °C by a cryostat. There the tars and steam condense. The liquid phases in the impinger bottles are unified and the aqueous phase is separated from the toluene phase. Afterwards, the amount of water is determined to calculate the water content in the gas stream. The amount of toluene is also marked down and a GC–MS sample is taken. Then the main part of the toluene is evaporated from the sample in a petri dish. To analyze the oil in the filter cartridge it is necessary to carry out a Soxhlet extraction with IPA. Again a GC–MS sample of the IPA phase is taken. Afterwards the IPA phase is handled like the toluene phase. The results of the toluene phase and the IPA phase are added, which gives the amount of gravimetric tar in the product gas. The filter cartridge is reduced to its ashes by oxidizing the organic matter in a furnace. By weighing the cartridge before and after the muffle furnace treatment, the amount of entrained char and dust can be calculated. Finally, the GC–MS sample is analyzed in a GC–MS device to determine the tar composition. This measurement method gave the following results:

- Gravimetric tar content
- GC–MS tar content
- GC–MS tar composition
- Water content
- Char load
- Dust load (inorganic matter).

3.2.3. NH_3 and H_2S measurement

For ammonia measurement, gas is sampled in a similar way to the sampling for the tar measurements, using impinger bottles. The solvent used in this procedure is diluted sulfuric acid at a temperature of about -2 °C. The impinger bottles are placed in a glycol/ethanol mixture whose temperature is cooled down by a cryostatic temperature regulator. To avoid tar condensation in the pump, a bottle with toluene is added after the solvent for NH_3. After this procedure the concentration of ammonium ions in the sulfuric acid can be detected by a photometric method according to DIN 38 406 Part 5 and ISO 7150. Hydrogen sulfide is sampled using impinger bottles filled with an aqueous potassium hydroxide solution at a temperature of about -2 °C. Subsequently, the H_2S values were determined by potentiometry.

3.2.4. Flue gas measurement

The composition of the flue gas was measured with a Rosemount NGA 2000 (CO, CO_2, and O_2).

3.2.5. Fuel analysis

The feedstock for the gasification tests is analyzed by the Testing Laboratory for Combustion Systems at Vienna University of Technology. The sampling and preparation of the fuels are done according to DIN 51701. After determination of the water content, described in DIN 51718 (drying at 30 °C to constant mass, grinding of the dried sample to a maximum particle size of 1 mm, and drying of this sample at 106 ± 2 °C in an inert atmosphere to constant mass), the ash content is determined according to DIN 51719 by burning the sample to constant mass. C, H, N, and S are measured by an EA 1108 CHNS-O elementary analyzer made by Carlo Erba. This is carried out by burning the sample under oxygen atmosphere. To make sure that CO formation is avoided, the gas passes a tungsten catalyst that ensures complete oxidation. Afterwards the gas passes a layer of copper at a temperature of 860 °C where free oxygen is bound. Here, nitrogen oxides are also reduced to N_2. As a result the gas consists only of the components CO_2, H_2O, N_2, and SO_2 that can be detected. Chlorine present in the gas is absorbed in an aqueous perhydrol solution (H_2O_2) which is analyzed afterwards by capillary electrophoresis.

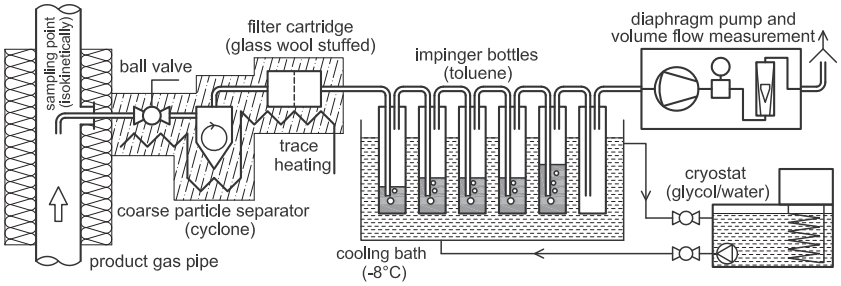

Fig. 3. Tar sampling line.

3.3. Balance of the pilot plant

All of the online measured values obtained during a gasification test are recorded by process-control software. Using the data collected, mass and energy balances of the DFB system can be calculated. For this purpose, the balance tool IPSEpro was used. IPSEpro is a stationary, equation-oriented flow sheet simulation tool that has been developed for power systems. Detailed information about IPSEpro, its mode of operation, and its utilization for biomass-based energy systems are published by Pröll and Hofbauer (2008).

3.4. Used bed material

The bed material that is used for the tests is olivine, provided by the Austrian manufacturer Magnolithe GmbH. As discussed before it has been observed that calcination of olivine before using it in the gasifier increases its catalytic potential. This thermal preparation is done by the manufacturer in a rotary kiln reactor at a temperature of up to 1600 °C for about four hours. Due to this the material is sintered. The results of the XRF analysis as can be found in Kirnbauer, Hofbauer (2011). Based on the sieve analysis of the bed material the particle diameter by this methodology was calculated to be $d_p = 411\ \mu m$. The shape of the olivine particles was identified as approximately spherical, so the way to specify the mean sauter diameter of the used bed material is $d_{sv} = \phi d_p$. With the sphericity $\phi = 0.9$ the mean sauter diameter results to $d_{sv} = 370\ \mu m$. This particle size is classified according to Geldart (1973) as particle group B.

3.5. Feedstock

Wood pellets produced according to the Austrian standard ÖNORM M 7135 are usually used as a standard fuel to represent wood in the gasifier. For the processing of biomass in a power plant, wood chips are mostly the designated fuel, but in the pilot plant the pieces have to be smaller and the quality of the fuel has to be held constant for the entire test campaign. Therefore, instead of wood chips, wood pellets are normally used for the tests. Furthermore, it was found during previous tests that wood pellets behave similarly to wood chips in the DFB gasifier (Kirnbaueret al., 2012). Proximate and ultimate analyses of the used wood pellets are listed in Table 2.

4. Results and discussion

4.1. Overview

Gasification of wood was carried out at two different operating points (OP1 and OP2). The general parameters of these tests are summarized in Table 3. In addition, to investigate the general performance and the product gas composition of steam gasification of wood pellets, a further objective of these test series is to study the influence of the position where the fuel is fed into the gasification reactor on the performance of the system and the reactions in the freeboard of the gasifier. Both gasification tests were accomplished with a fuel power of 90 kW, which corresponds to a mass flow rate of wood pellets of 18.6 kg/h. For gasification test OP1, the wood pellets were fed into the bubbling bed, whereas for OP2 the wood pellets were introduced into the freeboard of the gasifier where the pellets drop onto the surface of the bubbling fluidized bed of hot olivine particles. Both test runs were operated with the same key data for gasification, that is, the same gasification temperature, bed material size and type,and steam-to-fuel ratio ($\varphi_{SF} = 0.6\ kg_{H_2O}/kg_{daf}$),which represents the steam present in the gasifier that will act as the gasification agent. For each test a new batch of 100 kg of olivine was used. Tar was sampled at each operating point whereas H_2S and NH_3 were only sampled at OP1 as their release into the product gas is relatively constant if the same feedstock is used and the gasification temperature is not affected.

The steady state phase was held between 7 and 9 h for both operating points. This long time period was necessary as the discontinuous sampling methods had to be done one after another, to get the opportunity to observe any interactions in the system that produce a certain trend in the gas composition and the process performance and to get a sufficient amount of data to close all balances. For start-up of the system, both reactors are operated in combustion mode (fluidization with air). When the temperatures for operation are reached, the fluidization agent for the gasification reactor is changed to steam.

4.2. Key data and general gasification results

A first insight into the gasification behavior of wood pellets in the DFB system can be made by highlighting the temperatures in the gasifier at the different operating points and fluidization conditions in the system. An overview of the fluidization regime is presented in Table 4. The velocities U_{mf} and U_t and their ratios with the actual superficial velocity in the gasification and combustion reactors can be used for characterization of the fluidized bed system. The generalized regime map of gas–solid fluidized beds proposed by Grace (1986), Haider and Levenspiel (1989),

Table 4
Fluidization velocities and their ratios to minimal required values.

Value	Unit	OP1	OP2
Minimum fluidization velocity, U_{mf}	m/s	0.07	0.07
Terminal velocity, U_t	m/s	3.36	3.36
Superficial velocity gasification reactor, U_g	m/s	0.41	0.47
Fluidization number gasif. reactor, U_g/U_{mf}	–	5.69	6.53
Transport number gasif. reactor, U_g/U_t	–	0.12	0.14
Superficial velocity comb. reactor, U_C	m/s	8.9	9.0
Fluidization number comb. reactor, U_C/U_{mf}	–	124.1	124.5
Transport number comb. reactor, U_C/U_t	–	2.66	2.67

Table 3
General parameters for the gasification tests.

Value	Unit	OP1	OP2
Fuel feeding position	–	In bubbling bed	On bubbling bed
Fuel power wood pellets	kW	90	
Gasification temperature bubbling bed	°C	850 ± 2	
Mean temperature combustion reactor	°C	890	912
Fuel mass flow (wood pellets)	kg/h	18.60	
φ_{SC}	kg_{H_2O}/kg_{carbon}	1.3	
φ_{SF}	$kg_{H_2O}/kg_{fuel,daf}$	0.6	
Initial bed material inventory	kg	100	

and Abba et al.(2003) is used to illustrate the position of the operating points (Fig. 4).The *Y*-axis in this diagram represents the dimensionless velocity U* and the *X*-axis plots the dimensionless particle size d_P*. The values for Fig. 4 can be calculated by

$$d_P^* = Ar^{1/3} \tag{17}$$

$$Ar = \frac{\rho_g \cdot d_{sv}^3 \cdot \left(\rho_P - \rho_g\right) \cdot g}{\mu^2} \tag{18}$$

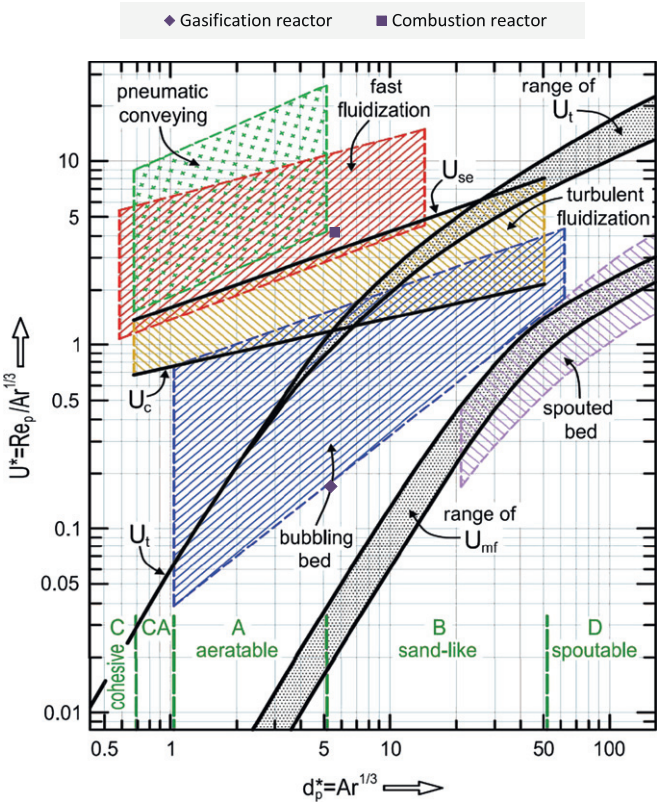

Fig. 4. Generalized fluidization regime map.

$$U^* = \frac{Re_p}{Ar^{1/3}} \tag{19}$$

$$Re_P = \frac{\rho_g \cdot U_S \cdot d_{sv}}{\mu} \tag{20}$$

The values for the gasification and combustion reactors are calculated for the mean sauter diameter of the bed material particles d_{sv}. In the gasification reactor the bubbling fluidized bed is operated with a value of U* that is relatively low but still around six times higher than U_{mf}. The fluidization regime in the combustion reactor has to be above the terminal velocity for a single particle (U_t), but for practical operation of the riser it should be above the superficial velocity where significant entrainment of solids occurs (U_{se}), and this criterion is fulfilled with the chosen operating points. The temperature profile in the gasification reactor for both operating points is shown in Fig. 5. This diagram shows that the temperatures over the height of the reactor differ from each other due to several impacts on the system. The hot bed material which transports the heat from the combustion reactor to the gasification reactor is circulated to the gasification reactor in the lower freeboard section. This causes a local hot spot where the highest temperature in the reactor is measured. Where the superheated steam for fluidization is introduced into the bubbling bed, a cold spot is produced, because the steam temperature is about 300 °C, which is significantly lower than the bed material temperature (≈ 850 °C). But due to good intermixing of steam, bed material, and fuel particles and the high heat capacity of the bed material, the temperature decrease is limited. The set point for the gasification temperature (850 °C) is chosen at the height in the middle of the bubbling bed. In this area the fuel is fed into the gasifier in case of OP1. In the middle and upper sections of the freeboard, the temperature drops slightly in a constant way due to heat losses and energy-consuming reactions like steam reforming and cracking reactions as well as pyrolysis and gasification of any particles entrained in the freeboard.

With the temperature profiles of the gasification test, a first estimation of the behavior of the system can be made. The gasification temperature was controlled to 850 °C. To reach this, the recirculated bed material had to provide a much higher temperature in the case of OP2, where on-bed feeding of the

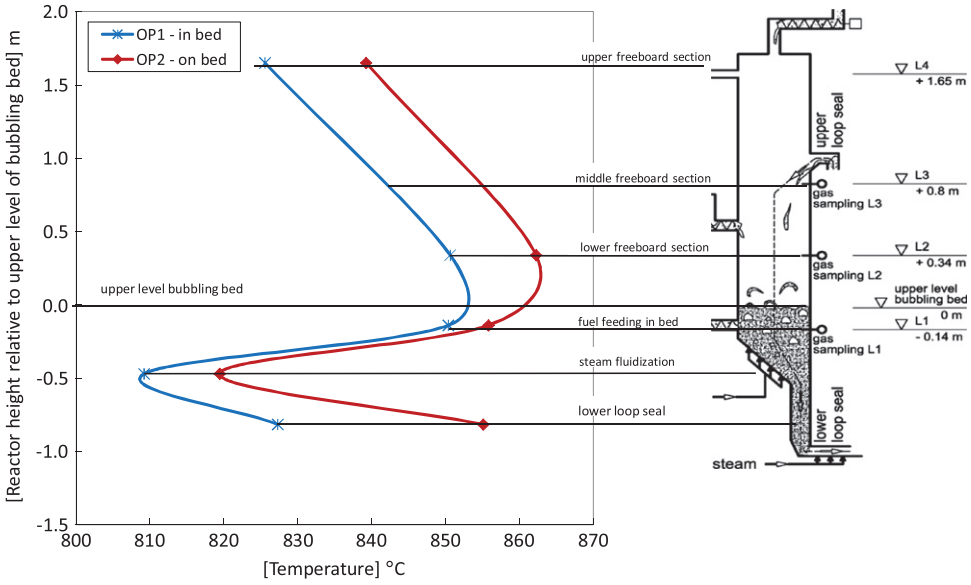

Fig. 5. Temperature profile in the gasification reactor.

solid feedstock was applied. As a result, the highest temperature in the freeboard was reached for OP2 and was about 12 °C higher compared to feeding the feedstock into the bubbling bed. The cold spot in the surroundings of the steam fluidization was affected more during OP1, where the temperature was cooled down to 810 °C, while for OP2 a temperature of 820 °C was recorded at this point. The more intense cooling was a result of the fuel particles being heated up, dried, and pyrolyzed; some of them were also gasified in this zone: all of these four steps of fuel conversion are energy consuming. For the case of OP2, where on-bed feeding of the pellets was applied, these steps took place to a large extent while floating in the area of the splash zone of the fluidized bed and cooled the particles only in a small part of the vertical height.

4.3. Product gas composition

The DFB gasification process yields two separate gas streams: a product gas stream (gasification reactor) and a conventional flue gas stream (combustion reactor). The product gas primarily consists of the gas components hydrogen (H_2), carbon monoxide (CO), carbon dioxide (CO_2), methane (CH_4), ethylene (C_2H_4), ethane (C_2H_6), and unconverted water (H_2O). The difference between the sum of these main components and 100% of the gas components is made up by the following components or impurities:

- A nitrogen (N_2) content < 1.5 vol%$_{db}$ can be present in the product gas as N_2 is used in the process as gas for inertization of the fuel feeding system.
- Gaseous C_2–C_5 hydrocarbons that are not detected with the applied measurement devices.
- Hydrogen sulfide (H_2S) in the product originating from the sulfur content in the fuel.
- Ammonia (NH_3) in the product originating from the nitrogen in the fuel.

Mean values of the main permanent gas components are summarized in Fig. 6,which provides a good impression of the influence of the feeding position on the gas composition. As mentioned before, Gómez-Barea et al. (2013) concluded that a fuel feeding position above a bubbling bed produces a gas that shows more characteristics of a pyrolysis gas, namely a lower H_2 content and higher contents of higher hydrocarbons and tar. This behavior can also be seen here. With fuel feeding into the bed (OP1) the product gas consists of 39.3 vol%$_{db}$ H_2, 30.5 vol%$_{db}$ CO, 16.2 vol%$_{db}$ CO_2, 9.3 vol%$_{db}$ CH_4, and 1.9 vol%$_{db}$ C_2H_4. In contrast to this, forOP2 only 32.8 vol%$_{db}$ H_2 and 14.6 vol%$_{db}$ CO_2 were detected but CH_4 increased up to 10.3 vol%$_{db}$ and C_2H_4 was found to be 2.7 vol%$_{db}$ in the product gas. By the specific production of the gas components presented in Table 5, a more exact

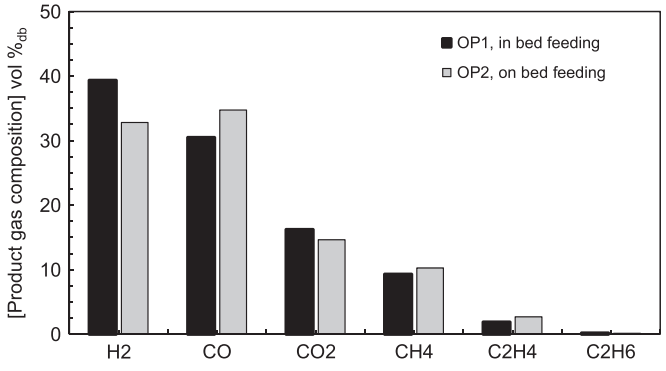

Fig. 6. Measured permanent gas composition of the product gas.

Table 5
Specific production of the main gas components.

Value	Unit	OP1	OP2
Specific H_2 yield	$Nm^3_{H2}/kg_{fuel,daf}$	0.408	0.374
Specific CO_2 yield	$Nm^3_{CO2}/kg_{fuel,daf}$	0.168	0.167
Specific CO yield	$Nm^3_{CO}/kg_{fuel,daf}$	0.316	0.396
Specific CH_4 yield	$Nm^3_{CH4}/kg_{fuel,daf}$	0.096	0.117
Specific C_2H_4 yield	$Nm^3_{C2H4}/kg_{fuel,daf}$	0.019	0.031
Specific C_2H_6 yield	$Nm^3_{C2H6}/kg_{fuel,daf}$	0.002	0.002

Table 6
GC–MS tar components that were found only for OP2.

Component	Unit	OP2
Benzo[a]pyrene	mg/Nm^3	99.80
Dibenz[a,h]anthracene	mg/Nm^3	99.46
Carbazole	mg/Nm^3	27.38
4-Methylphenol	mg/Nm^3	23.68
Isoquinoline	mg/Nm^3	13.83
1-Benzothiophene	mg/Nm^3	11.10
Indole	mg/Nm^3	1.90

determination of the change in the components produced can be provided. The specific amount of H_2 decreased by about 8.2% forOP2 compared to OP1. The highest increase in the specific amounts produced was ascribed to ethylene (C_2H_4),which showed an increase of 58% for OP2 compared to OP1.The production of carbon monoxide (CO) increased by about 25% and that of methane (CH_4) by about 21%. The relatively high increase in C_2H_4 is caused by the very low total amount produced forOP1. C_2H_6 was almost unaffected as its share in the product gas was very low.

The higher production of methane and higher hydrocarbons also has an influence on the heating value of the product gas (Table 7) as this value increased in the gas produced by feeding the fuel above the bubbling bed (OP2). From the results of the specific production of the permanent gas components, it can be estimated that the total product gas amount increased with on-bed feeding, as shown in Fig. 7. An explanation for this could be that the residence time of the char particles in the gasification reactor is increased in OP2 as the possibility that a char particle will move together with the bed material to the combustion reactor through the lower loop seal is higher when the fuel is fed into the bubbling bed (OP1). This also results in a higher conversion rate of carbon in the gasification reactor to the gaseous products shown in Fig. 8. The higher conversion of water (gasification agent) with in-bed feeding (Fig. 8) is due to the fact that the gasification reactions are faster in the presence of a catalyst like the hot solid olivine particles. With in-bed feeding (OP1) the olivine–char–steam system can drive the gasification reactions more easily and especially steam reforming reactions take place primarily in the bed zone. In the OP2 gasification test the pyrolysis gases are only able to react with the olivine particles and the steam in the small splash zone or in the freeboard without any catalytic action of the particles. With in-bed feeding much of the higher hydrocarbons was reduced by steam reforming in the bubbling bed. This is also a reason why the hydrogen content is higher and higher hydrocarbons are reduced with OP1. The most interesting aspect concerning the permanent gas composition of the product gas is the shift between H_2 and CO.

The steam-to-fuel ratio (φ_{SF}) chosen for the test runs here was low ($\varphi_{SF}=0.6$ $kg_{H_2O}/kg_{fuel,daf}$) compared with previous research activities at the pilot plant at Vienna University of Technology. In a previous research by Koppatz et al. (2011) the influence of the steam-to-fuel ratio (φ_{SF}) in steam gasification of wood pellets was

Table 7
Specific data of the accomplished tests.

Value	Unit	OP1	OP2
Total product gas yield	Nm^3/h	27.52	30.68
H_2O content in product gas	vol%	32.62	35.76
Dry product gas yield	Nm^3_{db}/h	18.09	19.88
Specific product gas yield	$Nm^3_{db}/kg_{fuel,daf}$	1.04	1.15
LHV	MJ/Nm^3_{db}	13.62	14.23
Syngas power $_{excl.\ tar}$	kW	68.40	78.60
Cold gas efficiency, $\eta_{c,IP}$	%	68.97	70.06
Logarithmic deviation from CO-shift equilibrium, $p\delta_{eq,CO\text{-}shift}$	–	−0.45	−0.49
Carbon conversion in the gasification reactor, X_C	%	66.85	82.31
Overall carbon conversion of the DFB system, $X_{C,DFB}$	%	96.62	97.19
Specific tar content, GC–MS	$g/kg_{fuel,daf}$	7.43	19.34
Specific tar content, grav.	$g/kg_{fuel,daf}$	1.54	11.18
Specific tar content, GC–MS	g/kg_{carbon}	14.75	38.39
Specific tar content, grav.	g/kg_{carbon}	3.06	22.19
Tar intensity per kWh of syngas, GC–MS	g/kWh_{syngas}	1.89	4.26
Tar intensity per kWh of syngas, grav.	g/kWh_{syngas}	0.39	2.46
Mean gas residence time freeboard gasifier, τ_F	s	3.77	4.15
Mean gas res. time combustion reactor, τ_C	s	0.86	0.85

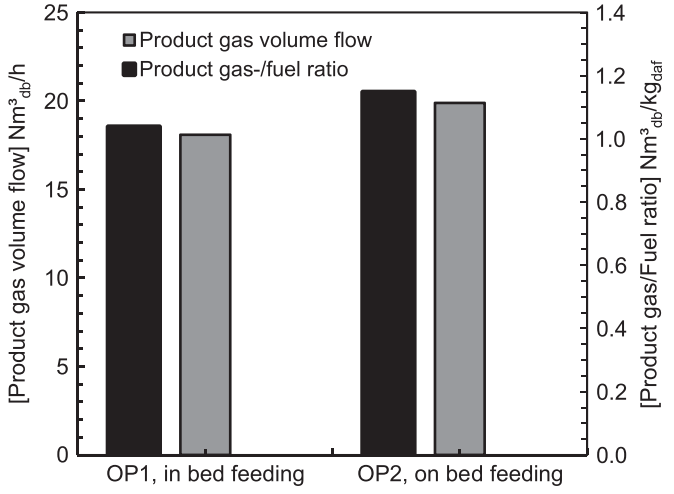

Fig. 7. Total and specific gas production.

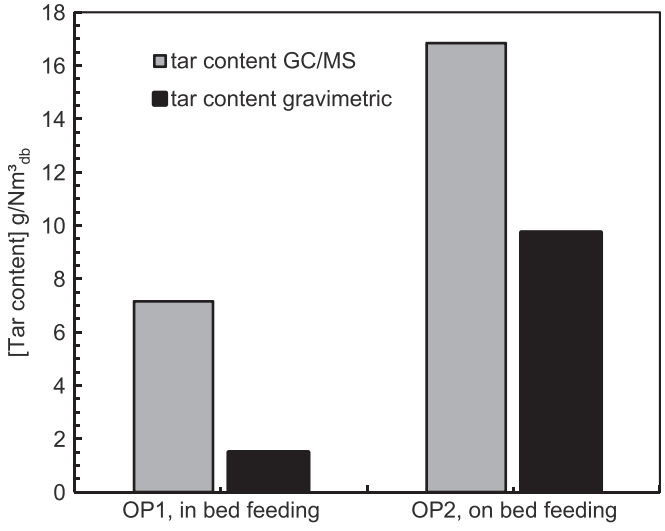

Fig. 9. GC–MS and gravimetric tar content in the product gas.

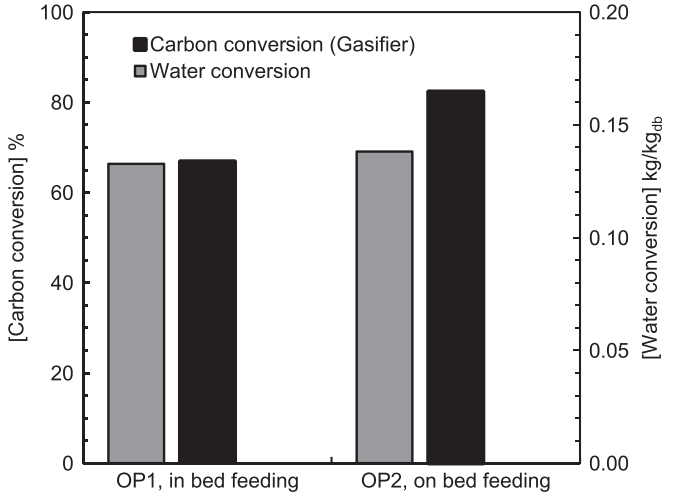

Fig. 8. Carbon- and water conversion in the gasification reactor.

studied and it was found that especially CO and CO_2 are influenced significantly if φ_{SF} drops below a certain value. For wood pellets this was when $\varphi_{SF} < 0.84\ kg_{H_2O}/kg_{fuel,daf}$. The reduction of φ_{SF} down to $0.74\ kg_{H_2O}/kg_{fuel,daf}$ caused an increase of CO and a decrease of CO_2 in the product gas. Only a minor effect was found for H_2 (a decrease when φ_{SF} was lowered) and CH_4 was not influenced significantly. In the case here the value of φ_{SF} is even lower so this effect is already even more distinctive forOP1. The sum of the effects explained before causes this difference in the gas composition.

The amounts of H_2S and NH_3 were measured only for operation of OP1 where 21.5 ppm_v of H_2S and 856.5 ppm_v of NH_3 were found. These impurities are formed by the sulfur and nitrogen content of the biomass. Previous research showed that nearly all of the introduced nitrogen is released in the gasification reactor [20, 24]. In a DFB gasifier it has been found that the release of H_2S in the product gas is between 50 and 90% of the amount of sulfur introduced while the rest leaves the system as SO_2 in the combustion reactor (Kern et al., 2011). Due to the higher residence time of the fuel particles in the gasification reactor with on-bed feeding of OP2 (explained before), it can be assumed that this percentage of released sulfur in the product gas will increase slightly, but in total volumetric numbers the H_2S content does not have to be higher as the amount of syngas produced is also higher and may dilute this sulfur content in the gas. Furthermore the measured H_2S content in the gas was already at a low level.

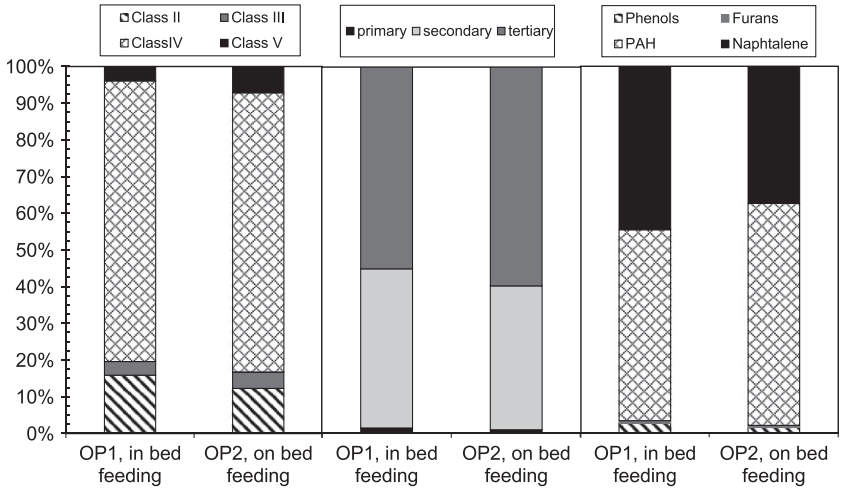

Fig. 10. GC–MS tar classification according to ECN (2009), Milne et al. (1998) and Wolfesberger et al. (2011).

4.4. Tar content

Especially for the downstream installations of utilization of the product gas, the tar content is a most crucial value. For each operating point, various tar samples were taken and analyzed according to their amounts, as shown in Fig. 9 (gravimetric tar and GC–MS tar), as well as the composition of the GC–MS tar presented in Fig. 10 and Table 6. As expected, GC–MS tar as well as the gravimetric tar content increased massively in the product gas when the pellets were fed onto the bubbling bed. Compared to in-bed feeding, the GC–MS tar increased from 7.2 g/Nm^3_{db} up to 16.8 g/Nm^3_{db}, which corresponds to an increase of 135%. The effect on the gravimetric tar was even more drastic because these compounds in the product gas increased by about 555% (from 1.5 g/Nm^3_{db} for in-bed feeding up to 9.7 g/Nm^3_{db} for on-bed feeding). This massive increase in the gravimetric tars, consisting mainly of large compounds with a high molecular weight, strengthens the fact that the product gas of on-bed feeding shifts toward the character of a pyrolysis gas (Gómez-Barea et al., 2013). The individual tar components can be detected by GC–MS analysis. A classification of these tar components can be made according to several aspects. Milne et al. (1998) categorized the components into primary, secondary, and tertiary tar components depending on their temperature of formation. Another classification can be made when the individual components are dedicated to their super-ordinated groups (Wolfesberger et al., 2011). These groups are phenolic compounds, furans, aromatic compounds, and polyaromatic hydrocarbons (PAH). Naphthalene, as the most dominant and most stable tar component, would belong to the group of PAH. To make the content of naphthalene visible it will be removed from the group of PAH and treated separately. A third and widely used classification is the characterization according to ECN (2009). Here, tars are classified into five classes. Class I collects tars that are non-detectable by GC–MS as they condense at high temperatures (high molecular weight fraction of gravimetric tar). The other tar classes (II–V) are lighter hydrocarbons that are present in the tar. The complete classification of the individual GC–MS tar components into the classes discussed here can be found in Koppatz et al. (2011). The classification of the GC–MS tar components into these groups is shown in Fig. 10.

From these data it can be seen that the relative contribution of naphthalene, as the most dominant GC–MS tar component, to the GC–MS tar decreased for OP2 compared to OP1 (Fig. 10). Further components whose shares decrease are indene and phenols. In contrast to this, the share of components like anthracene, fluoranthene and benzo[g,h,i]perylene increased for in-bed feeding. On the other hand there were also substances found in the tar with on-bed feeding of the feedstock that were not present with in bed-feeding. These are listed in Table 6.

4.5. Conversion performance

Summarizing the tests, some characteristic values are listed in Table 7. As mentioned before, the water conversion was better for OP1 where the fuel was fed into the bed. This caused a reduced amount of water in the product gas for OP1 compared with OP2. To provide a value for the efficiency of the gasification system, the cold gas efficiency is used here. For calculation of this value in the case of tests on the pilot plant it has to be kept in mind that a pilot plant usually does not reach a low values of heat losses like an industrial large scale plant does. In the case of the DFB pilot plant the heat losses are nearly 20% of the fuel input. A large scale plant can be operated with significantly lower heat losses. Stidl (2012) calculated the heat losses by radiation for the main parts of the 10 MW_{th} DFB gasification plant in Oberwart, Austria (Kotik, 2010). Based on the reported heat losses, the heat loss by radiation for an industrial plant can be assumed to be 2% of the input fuel power. To compare the cold gas efficiency to other plants, it is calculated for an industrial plant size according to

$$\eta_{C,IP} = \frac{\dot{V}_{PG} \cdot LHV_{PG}}{(P_{fuel,G} + P_{fuel,C} - \dot{Q}_{PP}\dot{Q}_{IP})3600} \tag{21}$$

The distance to equilibrium of the water–gas shift reaction is on the side of the reactants for both operating points because $p\delta_{eq,CO-shift} < 0$. For on-bed feeding the reaction is even more on the side of CO and H_2O. Basically this is caused by the relatively low content of H_2 and relatively high content of CO in the gas, especially for OP2. Due to the missing gas–solid contact that enhances the reaction, the residence time of the gas in the freeboard (τ_F) is too short to favora better conversion to H_2 and CO_2.

To give further information about the possible result of the influence of the water–gas shift reaction on the gas composition, the gas composition for fulfilled water–gas shift equilibrium is displayed in Fig. 11. As discussed before, OP2 yields a higher product gas output with a higher heating value. Therefore more carbon from the fuel is converted to product gas. This can be explained by the fact that the possibility of a char particle leaving the gasification reactor at the bottom together with the bed

material is lower when the feedstock is fed onto the bed. A graphic illustration of these energy flows is shown in Fig. 12 for OP1 and Fig. 13 for OP2. In both figures the energy streams of the input and output streams as well as the heat loss of the gasification reactor (without the combustion reactor) are shown. The input stream of wood pellets and the stream of char that leaves the gasification reactor to the combustion reactor are assumed to be chemical power. Power in terms of sensible heat is displayed in the stream of the fluidization agent (steam), the heat provided by the hot bed material from the combustion reactor, and the heat losses of the pilot plant. The hot product gas that leaves the reactor is divided into a fraction made of chemical power and a fraction where sensible heat, entrained char, and tar are summed up, because the product gas is usually cleaned and cooled for further utilization and therefore only the chemical power is used as a product. Therefore often only the chemical energy can be used for the downstream processes. The heat from the combustion reactor $\Delta\dot{Q}_{DFB}$ is calculated as the difference in the sensible heat flows with the bed material from and to the gasification reactor. The most important aspect when comparing those two operating points is that, for OP1,24.6 kW of chemical power in the form of residual char leaves the gasification reactor and enters the combustion reactor whereas only about 10.9 kW of char are transported to the combustion reactor in case of OP2. This is in accordance with the increased power in the product gas. As nearly 15 kW of char are missing for the combustion reactor, this part has to be substituted with some more fuel (light heating oil in the case of the pilot plant) for combustion to close the balance and steadily provide the heat for the gasification process.

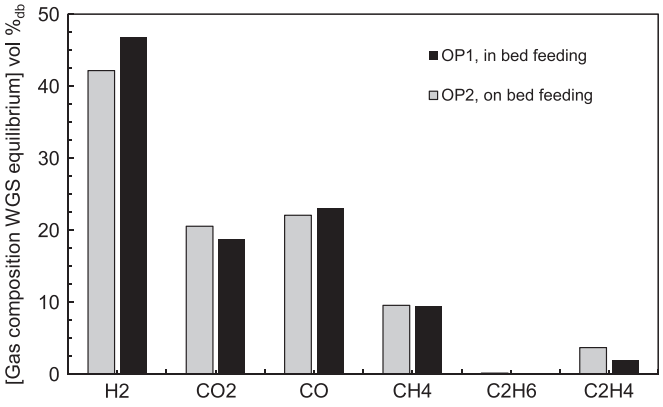

Fig. 11. Calculated gas composition for fulfilled water–gas shift equilibrium.

4.6. Product gas composition in the gasification reactor

As shown in Table 7, the mean gas residence time in the freeboard (τ_F) is around 4 s. τ_F is calculated considering a plug flow of the gas in the freeboard. To find out if and how the gas composition is affected in the freeboard of the gasifier, the permanent gas components H_2, CO, CO_2, CH_4, C_2H_4, and C_2H_6 were detected at three different levels in the gasifier in addition to the standard sampling point at the outlet of the gasifier. The gas analysis was carried out similarly to the standard permanent gas measurement methods (Rosemount NGA2000 and Perkin Elmer Clarus 500). The gas was sampled at two heights in the freeboard and one sampling point was chosen in the bubbling bed. The sampling points and their vertical heights, relative to the surface of the bubbling bed in the gasifier, are displayed in Fig. 5.

The caption of these points is also shown. L1 (level 1) is the sampling point in the bubbling bed which is 0.14 m below the bed surface. L2 (level 2) is located 0.34 m above the bubbling bed and L3 (level 3) is the sampling point at a vertical height of 0.8 m above the bubbling bed. L4 (level 4) represents the gas composition at the outlet of the reactor at a vertical height 1.65 m above the bubbling bed. For L4 the gas composition of the standard sampling (these values were discussed before) is used. Next to each sampling point (except L3) a thermocouple is also installed to precisely determine the temperature at the sampling point. The temperature profile of the gasification reactor is shown in Fig. 5. To avoid any reactions of the gas in the sampling pipe, the product gas was cooled down as fast as possible by a water cooled pipe. The gas was cooled down from the high temperature in the reactor to ambient temperature in less than 0.12 s. This cooling rate ($>$ 1000 K/sec) should be sufficient to avoid post-sampling reactions. Unfortunately L2 was not ready for measurements for the gasification test of OP2, where the fuel was fed onto the bubbling bed, so this sampling point was used only for OP1. With the data obtained, each gas component can be plotted depending on the sampling level. Figs. 14–16 show these measured values for each gas component. On the *Y*-axis of these diagrams the height of the gasification reactor relative to the

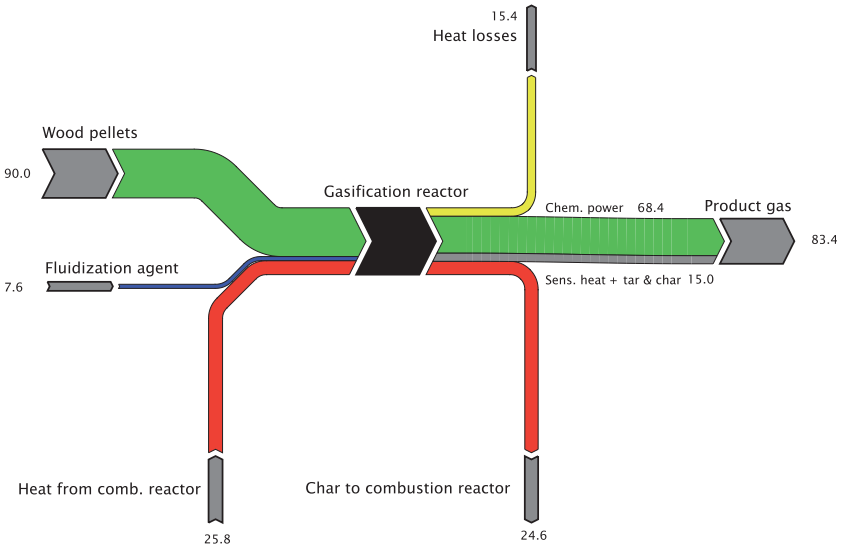

Fig. 12. Energy balance of the gasification reactor for in bed feeding (OP1), values in kW.

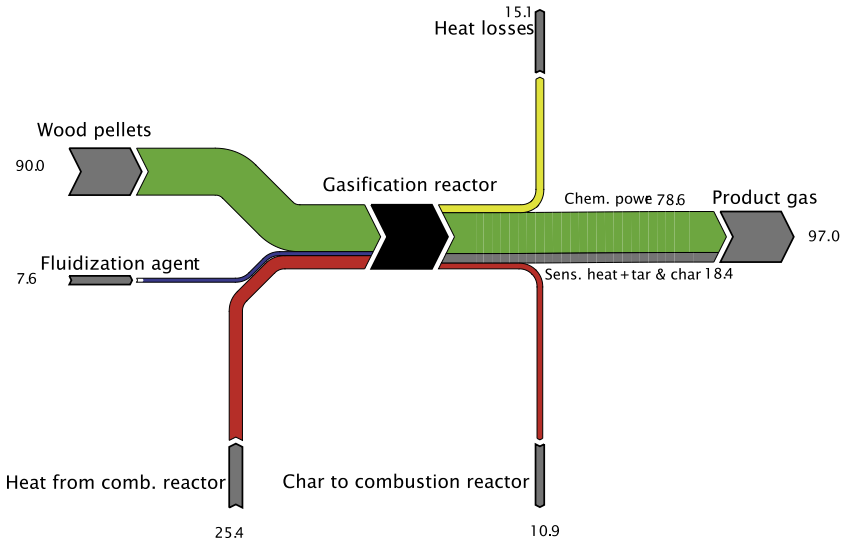

Fig. 13. Energy balance of the gasification reactor for on-bed feeding (OP2), values in kW.

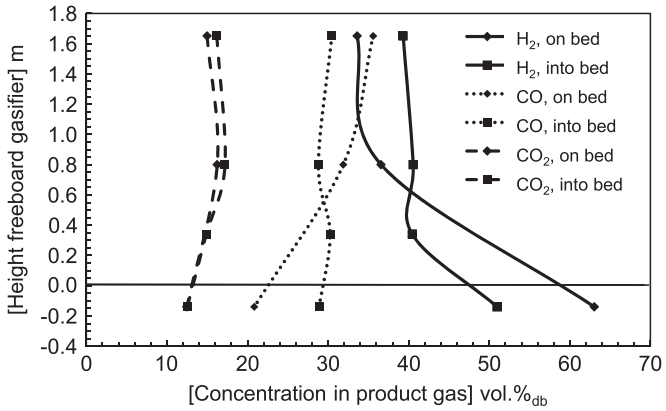

Fig. 14. H_2, CO and CO_2 profile in the gasification reactor.

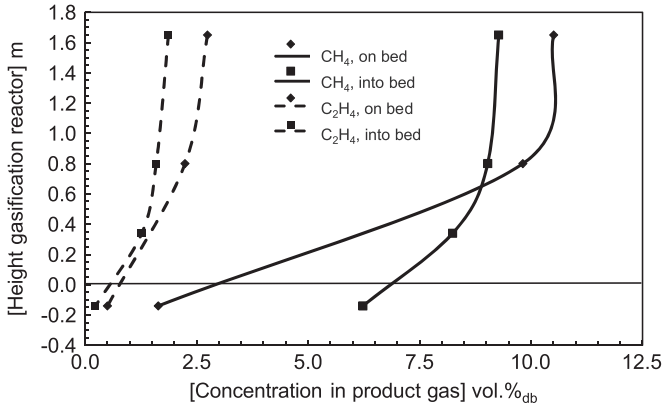

Fig. 15. CH_4 and C_2H_4 profile in the gasification reactor.

surface of the bubbling bed is listed. The black horizontal line in the diagram represents the height where the bubbling bed ends, so below this line is the bubbling fluidized bed of olivine particles and above it is the freeboard of the gasifier. Big differences in the gas composition can be observed depending on the vertical height. The most important aspect is that hydrogen increased up to 51 and 63 vol%$_{db}$ for OP1 and OP2 respectively at the lowest level. So due to an increase in the height, the H_2 content was reduced whereas the content of other gas components

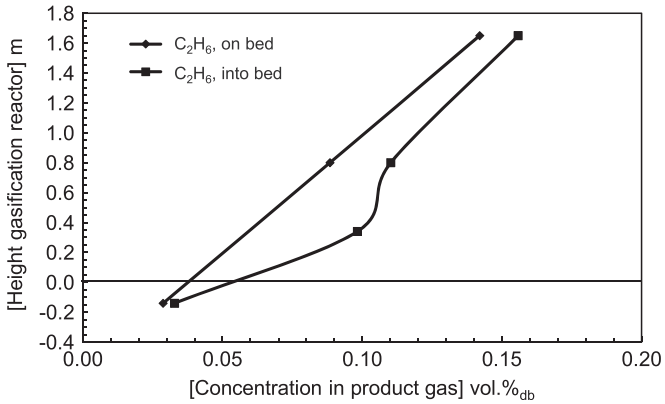

Fig. 16. C_2H_6 profile in the gasification reactor.

increased. This can be caused by the fact that the larger part of devolatilization of the fuel particles takes place in the upper area of the bubbling bed. Primary char and hot bed material are present in the bed, so a high H_2 content can be detected there, formed by the gasification reactions. If the pyrolysis gases are added to this gas amount, the H_2 content is reduced mostly in terms of dilution. This is the global aspect of these trends, which is much more distinctive in the case of on-bed feeding during OP2 than during in-bed feeding (OP1). This is because heating, drying, and devolatilization occur with on-bed feeding while most of the fuel particles float near the surface and the release of the gas is abrupt in a very small vertical height difference.

For the higher hydrocarbons C_2H_4 and C_2H_6 the profiles of the gas composition over the vertical height of the reactor showed a quite constant trend where C_2H_4 increased from 0.23 to 1.87 vol%$_{db}$ for OP1 and from 0.5 up to 2.75 vol%$_{db}$ for OP2. C_2H_6 was found in an even lower concentration but it also increased for higher sampling points in the freeboard. For both operating points, a concentration of 0.03 vol%$_{db}$ was detected at the lowest level (L1) while a mean C_2H_6 concentration of 0.15 vol%$_{db}$ was found at the top of the freeboard. The production of methane is influenced more than any other species in the freeboard by changing the feedstock feeding position. In Figure 22, it can be seen that in contrast to OP1, the concentration of CH_4 in the bubbling bed is marginal for OP2. When the wood pellets were fed onto the bed, only 15% of the final reactor outlet methane concentration was found at L1, while for the case where the pellets were fed into the bed, at L1 already 63%

of the final methane concentration was found. This strengthens the assumption that the larger part of the gas production process with woody biomass takes place in the bed when the fuel is fed into the bed whereas with on-bed feeding most of the gaseous products are generated in the upper level and the splash zone of the bubbling bed. The change in the CO_2 concentrations (Fig. 14) along the vertical height of the gasifier is, in relative numbers, not particularly noticeable; even the CO_2 content is nearly the same for both operating points at L1. The difference in the gasifier outlet concentration can be ascribed to the enhanced water–gas shift reaction at OP1. The content of carbon monoxide stayed more constant with in-bed feeding over the reactor height as shown in Figure 20. In addition to the missing contribution of the devolatilization products in the case of OP2, there is also a lower content of char present that drives the Boudouard reaction for the production of CO with char and the nearly constant content of CO_2 (Fig. 14) available. As was already discussed in Section 4.2, the temperature gradient also plays a role in influencing the gas composition. From L3 to the exit of the reactor the temperature decreases from the local hot spot of bed material recirculation. Above L3, the majority of the heterogeneous reactions and devolatilization processes of the feedstock particles should be finished and only homogeneous reactions should prevail with the exception of the gas–char reactions with entrained char. Entrained char was found in both cases in the range of 12–16 g/Nm^3_{db}. The increase of the gas components CH_4, C_2H_4, and C_2H_6 in the freeboard cannot be neglected (Figs. 15 and 16) from L3 to L4. The mean rise of the C_2H_6 content in relative numbers was about 50%. Also C_2H_4 increased by 19–23% in relative numbers in the tests and even the rise in CH_4 was around 5%. The water–gas shift reaction will not be dominant in the freeboard of the gasification reactor, as it was found before that only in the presence of a solid catalyst like olivine can influence the gas composition in a significant way. Some of these findings also agree with the measurements done by Miccio et al. (1999) for biomass gasification with air in a bubbling fluidized bed. He also documented an increase of the amount of CH_4 and higher hydrocarbons (C_2H_6–C_2H_8) found at higher levels in the freeboard and a higher total gas yield as the N_2 content decreased as height increased in the gasifier. The lower amount of H_2O found in the gas also strengthened this fact.

5. Conclusion

In this paper investigations on steam gasification of biomass was carried out at the Institute of Chemical Engineering at Vienna University of Technology with wood pellets, a fuel power of 90 kW, a gasification temperature of 850 °C, and a steam-to-fuel ratio (φ_{SF}) of 0.6 $kg_{H_2O}/kg_{fuel,daf}$ are presented. It was found that the position of feedstock admission has a significant impact on the product gas composition, amount, and quality. Also, the energy flow and the temperature profiles in the gasifier were affected. The major differences found in the case of feeding the feedstock onto the bubbling bed compared to in-bed feeding are

- Significantly higher CO content and lower H_2 content in the product gas.
- Water–gas shift equilibrium closer to reactants CO and H_2O.
- Higher amount of product gas.
- Higher carbon conversion in the gasification reactor.
- Lower water conversion.
- Higher tar yields (Seven new GC–MS tar species were found).

For the evaluation of the product gas quality and process performance the downstream utilization of the product gas has to be distinguished between heat and power production or synthesis processes and fuel cells. For heat and power production fuel feeding onto the bubbling bed (OP2) causes a higher efficiency of the whole process chain as the cold gas efficiency is higher in this case and the higher tar content does not cause problems if the gas does not have to be cooled below the dew point of the tars and is instantly burned in a boiler. If the product gas is used for synthesis processes or fuel cells, the product gas quality is an essential factor. Most of the synthesis processes like Fischer Tropsch-Synthesis or the production of CH_4 (SNG) require a H_2:CO ratio higher than 2 and a gas with a low amount of tars. The best fuel feeding design for this case is to feed the fuel directly into the bubbling bed as the gas composition is closer by the requirements (high H_2 content) of the downstream utilization of the product gas.

The feedstock feeding position also influences the profiles of the gas species in the gasification reactor. In general, the hydrogen content decreases as it passes along the freeboard towards the exit of the gasifier. This can be explained by the fact that in the bed some residual char forms primary H_2 and CO with the steam for gasification. The devolatilization products are released especially in the case of on-bed feeding at the top of the bubbling bed and are to a large part responsible for the dilution of hydrogen. The reactions in the freeboard are more distinctive when the solid feedstock is placed on the surface of the bed rather than in the splash zone, as drying and pyrolysis of these particles mainly occur in a very small vertical height range compared to the case when the fuel enters the bed in the middle of its height. In the latter case the pyrolysis products can already use the very intense gas–solid contact in the bubbling bed and react with the steam. These forced steam reforming reactions can also be seen as a part of the tar abatement and the lower content of higher hydrocarbons in this case.

Nomenclature

Symbols

Ar	Archimedes number, dimensionless
d_P^*	dimensionless particle diameter, dimensionless
d_P	general particle diameter, μm
d_{sv}	sauter diameter, μm
g	apparent gravity, m/s^2
$\Delta H_{R,850}$	heat of reaction at 850 °C, kJ/mol
$K_{p,\ CO^-shift}$	equilibrium constant of CO-shift, dimensionless
LHV_{PG}	lower heating value of the product gas (dry), MJ/Nm^3_{db}
$\dot{m}_{H_2O,actual}$	actual mass flux of steam in the gasification reactor, kg/h
$\dot{m}_{H_2O,stoich.}$	actual mass flux of steam in the gasification reactor, kg/h
$\dot{m}_{H_2O,steam}$	mass flux of steam in the gasification reactor, kg/h
$\dot{m}_{fuel}$	mass flux of solid fuel into the gasification reactor, kg/h
$\dot{m}_{H_2O,con.}$	amount of water that is converted to product gas, kg/h
$\dot{m}_{C_{PG}}$	carbon flux in the product gas stream, kg/h
P_i	actual measured gas phase partial pressure of the species i, Pa
$p\delta_{eq,CO-shift}$	logarithmic deviation from CO-shift equilibrium, dimensionless
$P_{fuel,G}$	input fuel power of solid fuel into gasification reactor, kW
$P_{fuel,C}$	input fuel power of fuel for combustion reactor, kW
$\dot{Q}_{PP}$	heat loss of the pilot plant, kW
$\dot{Q}_{IP}$	heat loss of an industrial size plant with the same power as the pilot plant, kW
Re	Reynolds number, dimensionless
T	temperature, °C
U^*	dimensionless gas velocity, dimensionless
U_{mf}	minimum fluidization velocity for a single particle, m/s
U_t	terminal velocity for a single particle, m/s
U_{se}	superficial velocity where significant entrainment of solids occurs, m/s

U_g, U_c superficial gas velocity in gasification reactor (g) and combustion reactor (c), m/s
$\dot{V}_{PG}$ volumetric flow rate of product gas (dry), Nm^3_{db}/h
$X_{H_2O,rel}$ water conversion in the gasifier, related to the fuel input, $kg_{H_2O}/kg_{fuel,daf}$
x molarity of carbon in the fuel (dry, ash, N, Cl, and S free basis), $mol/kg_{C,H,O}$
y molarity of hydrogen in the fuel (dry, ash, N, Cl, and S free basis), $mol/kg_{C,H,O}$
z molarity of oxygen in the fuel (dry, ash, N, Cl, and S free basis), $mol/kg_{C,H,O}$

Greek letters

δ deviation, dimensionless
ϕ sphericity, dimensionless
ϕ_{H_2O} stoichiometric H_2O demand, $mol_{H_2O}/kg_{daf,\ N,S,Cl\ free}$, $kg_{H_2O}/kg_{daf,\ N,S,Cl\ free}$
η_C cold gas efficiency, dimensionless
$\varphi_{SF,wt}$ steam-to-fuel ratio, $kg_{H_2O}/kg_{fuel,daf}$,, dimensionless
$\varphi_{SC,wt}$ steam-to-carbon ratio, kg_{H_2O}/kg_C, dimensionless
$\varphi_{SC,mol}$ molar steam-to-carbon ratio, mol_{H2O}/mol_C, dimensionless
λ_{H_2O} stoichiometric H_2O ratio mol/mol, kg/kg
μ absolute/dynamic viscosity, kg/(ms)
ρ_g gas density, kg/m^3
ρ_p density of a solid particle, kg/m^3
τ_F product gas residence time in the freeboard of the gasification reactor, s
τ_C gas residence time in the combustion reactor, s
ν_{ash} ash mass fraction in the fuel, dimensionless
ν_C carbon mass fraction in the fuel, dimensionless
ν_{H_2O} water mass fraction in the fuel, dimensionless

Abbreviations and subscripts

BTX benzene, toluene, xylene
c carbon, cold gas (efficiency), combustion reactor
CHP combined heat and power plant
daf dry and ash free basis
db dry basis
DFB dual fluidized bed
F freeboard
g gasification reactor
GC–MS gas chromatography mass spectrometry
IPA isopropanol
OP operating point
PAH polycyclic aromatic hydrocarbons
PG product gas
SNG substitute natural gas
sv surface volume

Acknowledgments

The authors gratefully acknowledge the financial support granted by the European Commission as this study was carried out within the framework of the Fecundus project, funded by the Research Fund for Coal and Steel of the European Union (Contract no. RFCR-CT-2010-00009).

References

Abba, I.A., Grace, J.R., Bi, H.T., Thompson, M.L., 2003. Spanning the flow regimes: Generic fluidized-bed reactor model. AIChE J. 49, 1838–1848.

Corella, J., Toledo, J.M., Molina, G., 2008. Biomass gasification with pure steam in fluidized bed: 12 variables that affect the effectiveness of the biomass gasifier. Int. J. Oil Gas Coal Technol 1, 194–207.

Devi, L., Craje, M., Thüne, P., Ptasinski, K.J., Janssen, F.J.J.G., 2005. Olivine as tar removal catalyst for biomass gasifiers: Catalyst characterization. Appl. Catal. A: Gen 294, 68–79.

ECN, 2009. Tar classification system. 〈http://www.thersites.nl〉.

Geldart, D., 1973. Types of gas fluidization. Powder Technol. 7, 285–292.

Gómez-Barea, A., Ollero, P., Leckner, B., 2013. Optimization of char and tar conversion in fluidized bed biomass gasifiers. Fuel, 103, 42–52.

Grace, J.R., 1986. Contacting modes and behavior classification of gas–solid and other two-phase suspensions. Can. J. Chem. Eng. 64, 353–363.

Green Paper, 2006. A European Strategy for Sustainable. Competitive and Secure Energy. Commission of the European Communities, Brussels.

Gunnarsson, I., 2010. The GoBiGas project—efficient transfer of biomass to biofuels. In: Proceedings of the International Seminar on Gasification, Gothenburg, Sweden, 28–29 October.

Haider, A., Levenspiel, O., 1989. Drag coefficient and terminal velocity of spherical and nonspherical particles. Powder Technol 58, 63–70.

Hofbauer, H., Rauch, R., Loeffler, G., Kaiser, S., Fercher, E., Tremmel, H., 2002. Six years experience with the FICFB-gasification process. In: Palz, W., Spitzer, J., Maniatis, K., Kwant, K., Helm, P., Grassi, A. (Eds.), Proceedings of the 12th European Biomass Conference, ETA Florence, Italy, pp. 982–985.

Hofbauer, H., Rauch, R., Bosch, K., Koch, R., Aichernig, C., 2003. Biomass CHP plant Güssing—A success story. In: Bridgewater, A.V. (Ed.), Pyrolysis and Gasification of Biomass and Waste. CPL Press, Newbury, Berks., UK, pp. 527–536.

HSC, HSC Chemistry 5.1, 2002. Outokumpu Research Oy, Pori, Finland.

Kaltschmitt, M., Hartmann, H., Hofbauer, H., 2009. Energie aus Biomasse. Springer, Berlin, Heidelberg.

Kern, S., Pfeifer, C., Hofbauer, H., 2011. Dual fluidized-bed steam gasification of solid feedstock: Matching syngas requirements with fuel mixtures. In: Luckos, T., den Hoed, P. (Eds.), Proceedings of the Industrial Fluidization South Africa (IFSA 2011), November 2011, Johannesburg, South Africa, 2011, pp. 67–78.

Kern, S., Pfeifer, C., Hofbauer, H., 2012a. Synergetic utilization of renewable and fossil fuels: dual fluidized bed steam co-gasification of coal and wood. APCBEE Procedia 1, 136–140.

Kern, S., Pfeifer, C., Hofbauer, H., 2012b. Co-gasification of wood and hard coal in a dual fluidized bed steam gasifier: process efficiency vs. gasification temperature. In: Proceedings of the 21st International Conference on Fluidized Bed Combustion (FBC), June 2012, Naples, Italy.

Kirnbauer, F., Hofbauer, H., 2011. Investigations on bed material changes in a dual fluidized bed steam gasification plant in Güssing, Austria. Energy Fuels 25, 3793–3798.

Kirnbauer, F., Wilk, V., Kitzler, H., Kern, S., Hofbauer, H., 2012. The positive effects of bed material coating on tar reduction in a dual fluidized bed gasifier. Fuel 95, 553–562.

Kitzler, H., Pfeifer, C., Hofbauer, H., 2011. Gasification of reed in a 100 kW dual fluidized bed steam gasifier. In: Proceedings of the 19th European Biomass Conference and Exhibition, June 2011, Berlin, Germany, pp. 1101–1105.

Klotz, T., 2010. A regional energy-supply-showcase – the 15 MW fuel-power biomass gasification plant Villach. In: Proceedings of the International Seminar on Gasification, Gothenburg, Sweden, October 28–29.

Koppatz, S., Pfeifer, C., Hofbauer, H., 2011. Comparison of the performance behaviour of silica sand and olivine in a dual fluidised bed reactor system for steam gasification of biomass at pilot plant scale. Chem. Eng. J. 175, 468–483.

Kotik, J., 2010. Über den Einsatz von Kraft-Wärme-Kopplungsanlagen auf Basis der Wirbelschicht-Dampfvergasung fester Biomasse am Beispiel des Biomassekraftwerks Oberwart. Ph.D. Thesis, Vienna University of Technology (written in German).

Miccio, F., Moersch, O., Spliethoff, H., Hein, K.R.G., 1999. Generation and conversion of carbonaceous fine particles during bubbling fluidised bed gasification of a biomass fuel. Fuel 78, 1473–1481.

Milne, T.A., Abatzoglou, N., Evans, R.J., 1998. Biomass Gasifier 'Tars': Their nature, formation, and conversion. National Renewable Energy Lab, Golden, CO, USA.

Molina, A., Mondragón, F., 1998. Reactivity of coal gasification with steam and CO_2. Fuel 77, 1831–1839.

Neft, J.P.A., Knoef, H.A.M., Zielke, U., Sjöström, K., Hasler, P., Simell, P.A., et al., 1999. Guideline for Sampling and Analysis of Tar and Particles in Biomass Producer Gases (Tar Protocol), ERK6-CT1999-20002 Version 3.1, ECN.

Pfeifer, C., Koppatz, S., Hofbauer, H., 2011a. Steam gasification of various feedstocks at a dual fluidised bed gasifier: Impacts of operation conditions and bed materials. Biomass Convers. Biorefin 1, 39–53.

Pfeifer, C., Koppatz, S., Hofbauer, H., 2011b. Catalysts for dual fluidised bed biomass gasification – an experimental study at the pilot plant scale. Biomass Convers. Bioref 1, 1–12.

Pröll, T., Hofbauer, H., 2008. Development and application of a simulation tool for biomass gasification based processes. Int. J. Chem. React. Eng. 6, 89.

Rapagna, S., Jand, N., Kiennemann, A., Foscolo, P.U., 2000. Steam-gasification of biomass in a fluidized-bed of olivine particles. Biomass Bioenerg 19, 187–197.

Schmid, J.C., Wolfesberger, U., Koppatz, S., Pfeifer, C., Hofbauer, H., 2011. Variation of feedstock in a dual fluidized bed steam gasifier – influence on product gas, tar content and composition. Environ. Prog. Sustain. Energy 31, 205–215.

Schuster, G., Löffler, G., Weigl, K., Hofbauer, H., 2001. Biomass steam gasification – an extensive parametric modeling study. Bioresour. Technol 77, 71–79.

Stidl, M., 2012. Prozesssimulation von spezifischen Anwendungsfällen der Zweibett-Wirbelschicht-Dampfvergasungs-Technologie für die Papier- und Zellstoffindustrie. Ph.D. Thesis, Vienna University of Technology, p. 112.

Wilk, V., Kern, S., Kitzler, H., Koppatz, S., Schmid, J.C., Hofbauer, H., 2011. Gasification of plastic residues in a dual fluidized bed gasifier – characteristics and performance compared to biomass. In: Proceedings of the International Conference on Polygeneration Strategies (ICPS11), Vienna, Austria.

Wolfesberger, U., Koppatz, S., Pfeifer, C., Hofbauer, H., 2011. Effect of iron supported olivine on the distribution of tar compounds derived by steam gasification of biomass. In: Proceedings of the International Conference on Polygeneration Strategies (ICPS11), 30 August–1 September, Vienna, Austria.

World Energy Outlook, 2010. International Energy Agency.

Zainal, Z.A., Rifau, A., Quadir, G.A., Seetharamu, K.N., 2002. Experimental investigation of a downdraft biomass gasifier. Biomass Bioenerg 23, 283–289.